International Journal of Thermal Sciences 171 (2022) 107239

Contents lists available at ScienceDirect

International Journal of Thermal Sciences

journal homepage: www.elsevier.com/locate/ijts

Thermal design parameters analysis and model updating using Kriging model for space instruments

Qinglong Cui [a,b], Guanyu Lin [a], Diansheng Cao [a,*], Zihui Zhang [a], Shurong Wang [c], Yu Huang [a]

[a] Changchun Institute of Optics, Fine Mechanics and Physics, Chinese Academy of Sciences, Changchun, Jilin, 130033, China
[b] University of Chinese Academy of Sciences, Beijing, 100049, China
[c] Foshan University, Foshan, 528225, China

ARTICLE INFO

Keywords:
Thermal simulation
Sensitivity analysis
Metamodel
Kriging
Model updating

ABSTRACT

In this study, we performed a thermal simulation analysis of a space instrument, a solar spectrometer. A thermal model updating method was used to introduce the Kriging model as the surrogated model into optimizing thermal design parameters instead of directly iterating the finite element analysis. The sensitivity analysis method was used to eliminate the insensitive parameters, thus determining the influence area of modeling parameters and saving processing time. The valid parameters were then used in Latin Hypercube Sampling (LHS) to generate training samples. Eight Kriging models were constructed by the training samples, and a Genetic Algorithm (GA) was used to find the optimal set of parameters, under which the temperature values at certain positions of the model were closest to the results of the heat balance experiment, thus updating the thermal model. The proposed method was successfully performed on the thermal design of a space instrument. Using this model, temperatures of specialized positions predicted by the updated model were more precise than the initial ones with the RMSE of temperature deviation of 0.88 °C. The surrogate model updating technology based on Kriging is rapid and efficient for the iterative thermal design of aerospace products.

1. Introduction

The extreme cosmic environment is the main constraint of the long-term safe operation of the space-borne experimental instruments [1]. Thermal radiation is a dominant heat transfer mode in space environments that does not support convection [2]. Thermal management of space instruments differs from the management of other devices. Besides alternating solar radiation and cold black background effects, heat generated by the instrument needs to be cleared to control the temperature in a reasonable range. As an important part of thermal design, thermal simulation technology is used to predict the temperature distribution of instruments during all phases, including the ground tests and the in-orbit environment. An accurate thermal simulation model has a key role in the designing, manufacturing, and operation of these payloads.

Usually, a thermal simulation model is not accurate enough. The modification of the model has always been a part of the thermal design of aerospace products. In the early phase of thermal design, the simulation model can only be modified by the trial and error method [3]. The development of finite element technology enables predicting the distribution of temperature by using the thermal finite element model (FEM), and the research is transferred to thermal FEM model updating. In Ref. [4], the random method was used to improve the efficiency of thermal model updating of the integral satellite; however, the correction accuracy was poor. Cheng et al. [5] modified the satellite thermal model by using the mixed Monte Carlo method. The deviation between the simulated temperature and the test temperature was within ±3 °C, which met the satellite thermal model correction requirements. Li and Chen [6] also used the Monte Carlo method to analyze the sensitivity of transient thermal model parameters of Carbon Dioxide Detector. Simplex Method was applied to classify parameters layer by layer, and the temperature error predicted by the modified model was less than ±0.5 °C.

The correction of the thermal model involves a repeated calculation of thermal FEM, which can be time-consuming and requires the development of a link program for software to realize the automatic correction process. Fortunately, the time of the process can be reduced by the metamodel technique known as an approximate model or surrogated model, which is a kind of mathematical expression abstracted from the complex FEM. A surrogate model can reduce the expensive calculation

* Corresponding author.
E-mail address: caodiansheng1987@163.com (D. Cao).

https://doi.org/10.1016/j.ijthermalsci.2021.107239
Received 9 January 2021; Received in revised form 22 July 2021; Accepted 17 August 2021
Available online 2 September 2021

cost by avoiding calculating FEM directly, thus making it more convenient to integrate the model into modifying process [7].

Model updating technology can be employed as an important method to calibrate FEM for mitigating modeling errors. The updated FEM may have the same behavior as the actual structure. After comparing the characteristics of the response surface method, neural network, and Kriging, Huang et al. [8] selected an adaptive Kriging to model the thermal simulation model of turbine disk and the Robust Archive Differential Evolution algorithm (RADE) to search the optimal solution of the model in the global range. Surrogate model updating technology is not limited to the optimization of design parameters. Moreover, Li et al. [9] constructed the critical vector surface k-RMS by Kriging and applied the model to Monte Carlo analysis. It made full use of the characteristics of the fast operation of the surrogate model and improved the analysis efficiency. In addition, Wang et al. [10] established a mathematical model for the impact response of the honeycomb sandwich panel structure. Kriging was used to construct the dynamic response model. The uncertain parameters in the modeling process were modified based on the experimental data due to simplification. The updated model results were highly consistent with the actual test results. Also, Shan et al. [11] used the response surface method to model FEM of a bridge. The model was updated by using the vibration test results and genetic algorithm to determine the equivalent stiffness of the contact area in the bridge.

Many researchers have specifically employed Kriging modeling strategies for numerical optimization [12–14]. Some engineering applications have provided elaborate discussions on structural design and dynamic simulation analysis. However, Kriging has shown limited application in aerospace engineering [15].

On the other hand, there are some discussions on parameter optimization of spacecraft thermal analysis model. NASA was the first to carry out the feasibility study of thermal network model modification, and made a deep research on the satellite thermal network modification method [16]. In the 1970s, S. Shimoji et al. [17] proposed the application of statistical regression method to modify the thermal network model. In the 1990s, Weng et al. [18] put forward a mixed correction method, using the transient thermal experiment results to modify parameters. Monte Carlo method is popular in recent years. In the study of Zhang et al. [19], the sensitive parameters were corrected by the means of Monte-Carlo mixed method according to the classification layer by layer. The transient temperature error is reduced from 8%~16% to less than 5%. The principle and calculation process of the correction methods above are usually complicated. Meanwhile, the research on parameter modification of the thermal simulation model has not formed the concept of establishing a mathematical model (surrogated model). If Kriging method is used to remodel the thermal FEM and the parameters are optimized on the surrogated model, process of model updating will be clearer and the calculation will be simplified. However, there is no research on thermal FEM optimization using surrogated model.

In this study, thermal simulation analysis of a space instrument, a solar spectrometer, was performed. In addition, the thermal FEM was modified by the surrogate model updating technique, thus making the temperature prediction of thermal FEM more accurate. The study has been divided into 5 sections: (1) background; (2) mathematical expression of Kriging, which is the theoretical basis of model construction; (3) design of experiment (DOE), which included the method of parameter selection, sampling, modeling, and testing; (4) objective function and method of updating; (5) case study. Firstly, the thermal FEM parameters of the solar spectrometer were analyzed. Then, the thermal FEM was modified with the data of the heat balance experiment. Finally, the accuracy of the updated model was evaluated. Conclusions are summed in the last section.

2. Mathematics aspect of the Kriging model

The term Kriging was initially used in the field of geography for stochastic process models. Volumes have been written on geostatistics [20,21] and spatial statistics [22,23], thus providing an excellent background on the development of the Kriging models as well as many practical applications. A Kriging model is a spatial interpolation model that offers both an expected value and uncertainty in that expected value.

The mathematical form of Kriging is shown in Eq. (1). It consists of a linear part and a nonparametric part. The first part, $\sum_{j=1}^{k}\beta_j f_j(\boldsymbol{X})$ is a simple linear regression of sampling points, which outlines the shape of the interpolation surface passing through the training points. The second part, $Z(\boldsymbol{X})$, is considered as the realization of a stochastic process [24], which "pulls" the response surface through the data by weighting the correlation of nearby points [25].

$$\hat{y}(\boldsymbol{X}) = \sum_{j=1}^{k}\beta_j f_j(\boldsymbol{X}) + Z(\boldsymbol{X}) \tag{1}$$

where $Z(\boldsymbol{X})$ is assumed to be a gaussian stationary process that follows normal distribution $N(0,\sigma_z^2)$ and has nonzero covariance as

$$Cov\left[z(x_i), z(x_j)\right] = \sigma_z^2 \boldsymbol{R} \tag{2}$$

where x_i and x_j are two training samples and $\boldsymbol{R}$ is a symmetry matrix composed by $R_{ij}(x_i, x_j)$.

$R_{ij}(x_i, x_j)$ can be specified by the user in some kind of correlation function that can characterize the correlation between any two training points. The function of $R_{ij}(x_i, x_j)$ is given by:

$$\begin{cases} R_{ij}(x_i, x_j) = \prod_{k=1}^{N_v} R_\theta(\theta_k, d_k) \\ d_k = \left| x_i^k - x_j^k \right| \end{cases} \tag{3}$$

where N_v represents the number of design variables; θ_k is the unknown coefficient of correlation; d_k is the distance between the different values of selected variables; x_i^k and x_j^k are the kth components of x_i and x_j, respectively. Therefore, the accuracy of the constructed Kriging model is determined by $R_{ij}(x_i, x_j)$.

Gaussian correlation function has wide application because of its smoothness characteristic [26], which is also employed in this study. The Gaussian correlation is defined as:

$$R_\theta(\theta_k, d_k) = \exp\left(-\theta_k d_k^2\right) \tag{4}$$

Detailed estimation of θ_k and σ_z can be found in Ref. [27]; σ_z is the function of θ_k. In simple terms, θ_k and σ_z can be evaluated by solving the maximum likelihood estimated problem as:

$$\max_{\theta_k > 0}\left(\frac{N_s \ln\left(\sigma_z^2\right) + \ln|\boldsymbol{R}|}{2}\right) \tag{5}$$

where N_s is the number of training samples and $|\boldsymbol{R}|$ is the determinant of $\boldsymbol{R}$, which is a function of θ_k.

θ_k is the most important parameter of the Kriging model. A model is constructed once the value of θ_k is given. The response at an untried position x_0 could be predicted by the model with unbiased estimation. The predicted response is written as:

$$\begin{cases} \hat{y}(\boldsymbol{x}_0) = \hat{\boldsymbol{\beta}} + \boldsymbol{r}^T(\boldsymbol{x}_0)\boldsymbol{R}^{-1}\left(\boldsymbol{Y} - \boldsymbol{F}\hat{\boldsymbol{\beta}}\right) \\ \hat{\boldsymbol{\beta}} = \left(\boldsymbol{F}^T\boldsymbol{R}^{-1}\boldsymbol{F}\right)^{-1}\boldsymbol{F}^T\boldsymbol{R}^{-1}Y \end{cases} \tag{6}$$

where $\boldsymbol{Y}$ is a column vector composed by the output of training points; $\boldsymbol{F}$ is a column vector filled with ones when $\boldsymbol{F}(\boldsymbol{x})$ is a constant vector; $\boldsymbol{r}(x_0)$ is a relevant vector composed between training points and predicted point x_0.

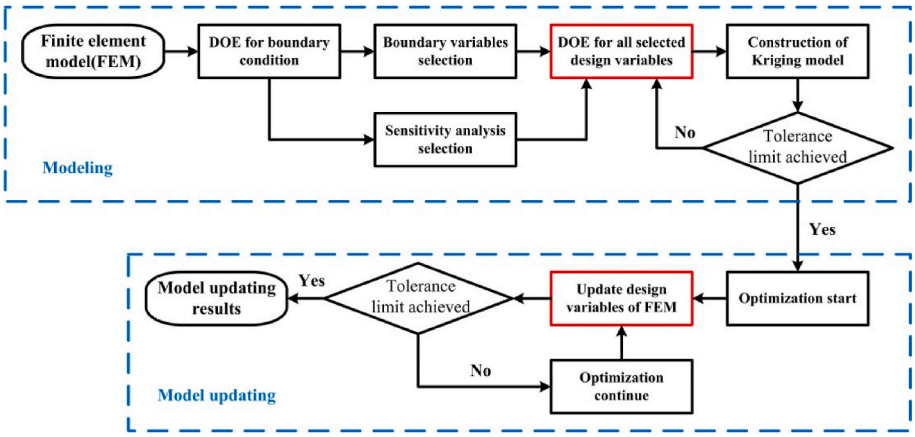

Fig. 1. Flow chart of the proposed modeling and model updating procedure.

$$\boldsymbol{r}(x_0) = [R_{01}(x_0, x_1), R_{02}(x_0, x_2), \ldots, R_{0Ns}(x_0, x_{Ns})]^T \tag{7}$$

Correlation parameters, $\boldsymbol{\theta}$, the process variance, $\boldsymbol{\sigma}^2$, and regression parameters, $\widehat{\boldsymbol{\beta}}$, are obtained through Maximum Likelihood Estimation (MLE), which makes them most consistent with the observed data. The method relies on the assumption that the observed data is the result of a gaussian process.

The likelihood function for a gaussian process is directly related to its probability distribution function given by:

$$L\left[\widehat{\boldsymbol{\beta}}, \boldsymbol{\sigma}^2, \boldsymbol{R}\middle|\boldsymbol{Y}\right] = \frac{1}{\boldsymbol{\sigma}^2\sqrt{|\boldsymbol{R}|(2\boldsymbol{\pi})^n}} e^{\frac{-1}{2\boldsymbol{\sigma}^2}\left(\boldsymbol{Y}-\boldsymbol{F}\widehat{\boldsymbol{\beta}}\right)^T \boldsymbol{R}^{-1}\left(\boldsymbol{Y}-\boldsymbol{F}\widehat{\boldsymbol{\beta}}\right)} \tag{8}$$

The logarithm of the likelihood function is taken for Eq. (8) is difficult to use. The estimate for $\widehat{\boldsymbol{\beta}}$ is calculated by taking the partial derivative of the log-likelihood function with respect to $\widehat{\boldsymbol{\beta}}$ and setting it to zero. Same as the generalized least squares estimate in Eq. (6), solving for the optimal variance yields:

$$\widehat{\boldsymbol{\sigma}}^2 = \frac{1}{n}\left(\boldsymbol{Y} - \boldsymbol{F}\widehat{\boldsymbol{\beta}}\right)^T \boldsymbol{R}^{-1}\left(\boldsymbol{Y} - \boldsymbol{F}\widehat{\boldsymbol{\beta}}\right) \tag{9}$$

Therefore the maximum likelihood estimates of $\widehat{\boldsymbol{\beta}}$ and $\widehat{\boldsymbol{\sigma}}^2$ are easily calculated if $\boldsymbol{R}$ is known. However, since $\boldsymbol{R}$ (·) is parameterized by $\boldsymbol{\theta} = \{\theta_1, \theta_2, \ldots, \theta_d\}$, the partial derivative of the likelihood function does not generally yield an analytic solution for $\boldsymbol{\theta}$ when set to zero. As a result, a constrained iterative search must be used. An optimization algorithm is often employed to select values for the correlation function parameters and evaluate the likelihood function using the optimal values for $\widehat{\boldsymbol{\beta}}$ and $\widehat{\boldsymbol{\sigma}}^2$, which themselves are functions of the correlation parameters [28].

3. Design of Experiment (DOE)

DOE is a scientific method for studying the relationship between multiple variables and the response, which helps to find out the ideal improvement scheme by selecting the experimental conditions, arranging a few experiments, and analyzing the experimental data.

In this study, DOE included two steps: first, the sensitivity analysis method was used to screen design parameters. Selected parameters were taken as variables in the second step. Training samples were then generated for constructing the Kriging model based on the variables in the second step. The flow chart of the proposed modeling and model updating procedure is shown in Fig. 1.

Thermal FEM is a simplified and idealized model with some uncertain parameters, such as the interface contact thermal resistance and thermal conductivity of composite materials. These parameters are variables that need to be optimized. The numerical range of each parameter is known according to the material characteristics and engineering experience, and the Latin hypercube sampling (LHS) method [29] is used to generate training samples.

The number of sampling needed for modeling is determined by the number of variables, and the number of training points is usually [10]

$$N = \frac{n(n+1)}{2} \tag{10}$$

where n is the number of the variables. Since every training point needs to be input into FEM to calculate the response value, more parameters and more training points need to be considered, thus longer modeling preparation work must be done. A thermal mathematical model requires many training points to obtain a more accurate response, which is not convenient. In that case, if the sensitivity analysis method [30] is used to screen the parameters, some parameters, which are not sensitive to the system response value, could be easily lost, in turn, greatly reducing the modeling time.

After modeling, the accuracy of the model needs to be verified. Similar to the sampling process, five inspection points (not the same as training points) are randomly selected to calculate the response value of the Kriging model. At the same time, the response values are compared with the response values of inspection points in FEM. If the difference between the responses is < 1 °C, the Kriging model is considered accurate. If the model error is out of tolerance at some inspection point, the inspection point is used as the new training point for remodeling until the response differences between Kriging and FEM at all inspection points are within the error range.

4. Model updating process

The relationship between the variables and the system response has been established in the modeling process, i.e., the relationship between thermal design parameters and the temperature at a specific position. The model updating process is intrinsically an inverse problem [31] and usually formulated as an optimization problem, aiming to minimize the differences between the FEM behavior and the corresponding experimental behavior.

Model updating generally requires an objective function to determine the update direction:

$$\min_{xiL<xi<xiU} \boldsymbol{O}, s.t. \quad i = 1, 2, \ldots, n \tag{11}$$

where $\boldsymbol{O}$ is the objective function; x_i is the design variables of the structure; x_{iL} and x_{iU} are the lower and upper bound of the input variables, respectively.

The objective function in this study is established based on the difference between the corresponding temperature of the Kriging model and the measured temperature in the experiment, which can be

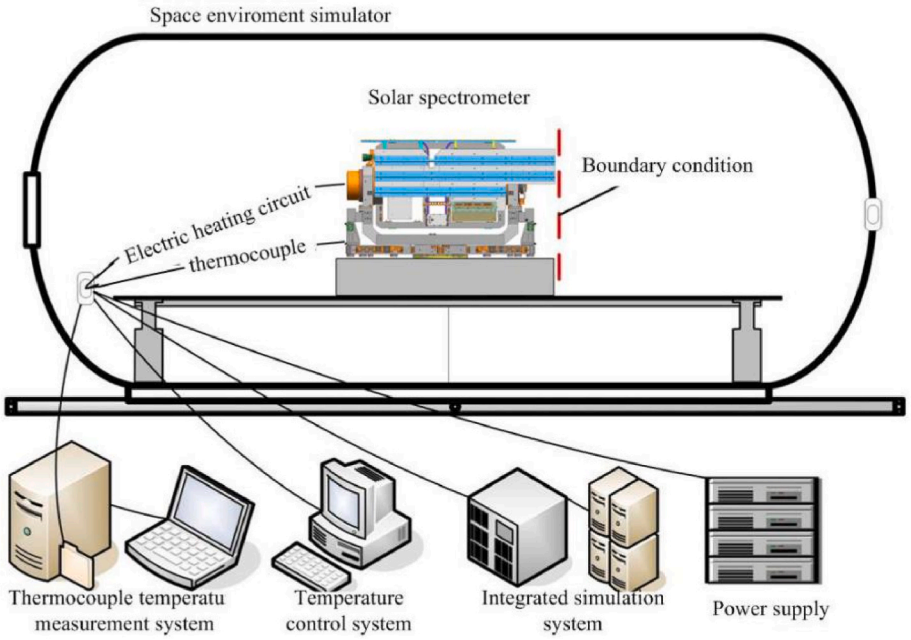

Fig. 2. Space environment simulator and peripheral devices.

formulated as follows:

$$O = \sum_{i=1}^{m} (TK_i - TF_i)^2 \tag{12}$$

where m is the number of measuring points; TK_i is the response value of the Kriging model based on the i-th measuring point; TF_i is the actual temperature value of the same position.

Genetic algorithm (GA) [32] is a kind of random search method which is based on the evolution law of Biology (survival of the fittest, survival of the fittest genetic mechanism). It is a search algorithm with the iterative process of "survival + detection". GA takes all individuals in a population as objects, and uses randomization technology to guide efficient search for a coded parameter space. selection, crossover and mutation are the three main data screening methods for GA. It directly operates on structural objects. For equations there is no requirement for continuity, nor derivation. As a global optimization search algorithm, GA has been widely used in various fields and achieved good results because of its feature of simple, strong robustness, high efficiency and practicality. These properties of GA have been widely used in combinatorial optimization, machine learning, signal processing, adaptive control and artificial life.

In the process of parameter optimization, GA is used to search for the optimal solution in the parameter boundary until a set of parameters is found, thus making the objective function value minimal. The model updating process is to find the set(s) of input combinations of the parameters that generate a pre-determined output, as shown in Fig. 1.

5. Case study

5.1. Thermal equilibrium experiment

The purpose of the thermal equilibrium experiment was to verify the correctness of the thermal design and check the working ability of the thermal control system in the space environment. By obtaining the temperature distribution data of space instruments under different working conditions, experimental results provide a reference for the subsequent optimization and modification of the thermal design model.

The test device is mainly composed of test pieces, boundary simulation components, space environment simulators, thermocouples. As shown in Fig. 2, the peripherals include a control system, comprehensive simulation equipment, power supply, and integrated simulation system. The solar spectrometer was placed in the space environment simulator during the test; other supplies were placed around the environment simulator and connected with the instrument through the warehouse cable.

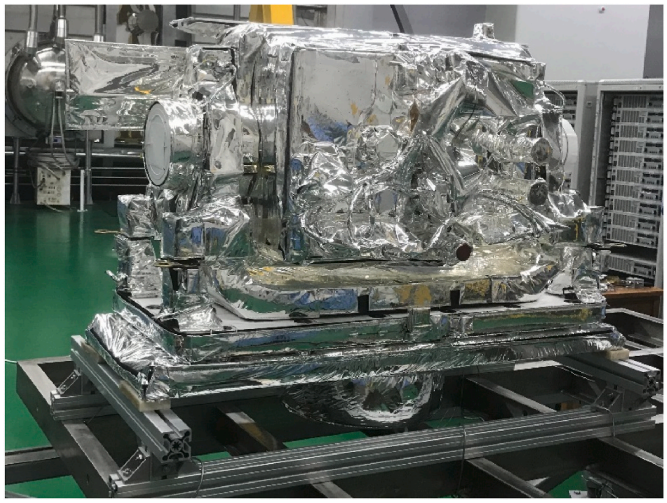

Fig. 3. Solar spectrometer.

The space environment simulator is a cylindrical sealed container with a diameter of 3 m, in which the heat sink is installed. The liquid nitrogen flows through the pipes in the heat sink and cools the ambient temperature to about −196 °C. Black paint is sprayed inside the vacuum container to simulate the cold black radiation environment in space, and the atmospheric pressure in the container is reduced to less than 10^{-4}Pa by a vacuum pump. Copper-constantan thermocouples with a resolution of 0.1 °C [33] is used to monitor the temperatures of some particular positions that are illustrated in the next chapter.

The space instrument, the solar spectrometer, is shown in Fig. 3. The outer surface of the instrument is covered with a multi-layer insulator (MLI) to isolate the alternating influence of the sun and the cold black

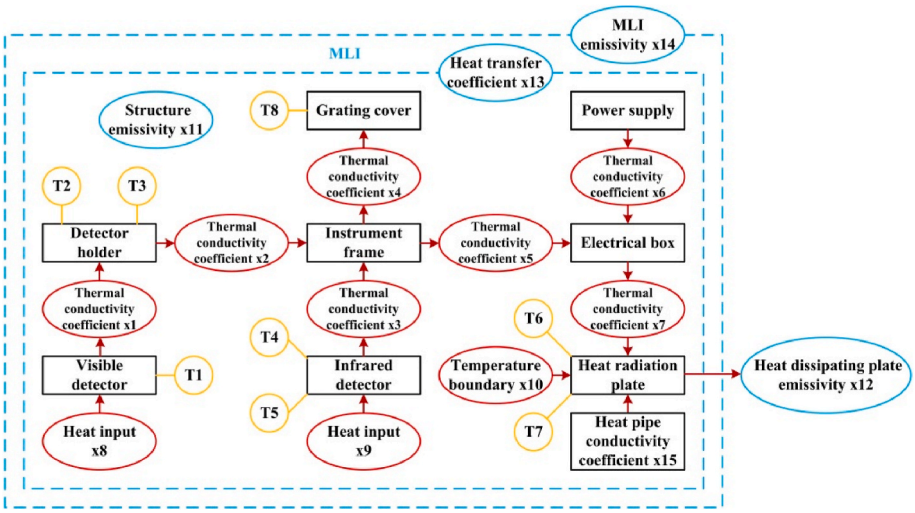

Fig. 4. Thermal equilibrium in surrounding environment for the instrument.

Table 1
Parameters along the heat transfer path.

Parameter	Description	Initial value	Range
x1	Thermal conduction coefficient between VIS detector and detector holder	2.3 W/°C	0.5–10 W/°C
x2	Thermal conduction coefficient between VIS detector holder and instrument frame	5 W/°C	0.5–15 W/°C
x3	Thermal conduction coefficient between the IR detector holder and instrument frame	5 W/°C	0.5–15 W/°C
x4	Thermal conduction coefficient between grating cover and instrument frame	0.1 W/°C	0.1–0.5 W/°C
x5	Thermal conduction coefficient between instrument frame and electrical box	4 W/°C	0.5–15 W/°C
x6	Thermal conduction coefficient between power supply and electrical box	1 W/°C	0.2–5 W/°C
x7	Thermal conduction coefficient between instrument frame and the radiation plate	1 W/°C	0.6–8 W/°C
x8	Active heating power of VIS detector	6 W	4–8 W
x9	Active heating power of IR detector	2 W	1–3 W
x10	Temperature boundary of instrument	−4 °C	−8~-2 °C
x11	Emissivity of structural surface	0.88	0.6–0.98
x12	Emissivity of the structural heat pipe	0.88	0.6–0.98
x13	Heat transfer coefficient between structure and MLI	0.1	0.02–0.5
x14	Out layer emissivity of MLI	0.69	0.5–0.98
x15	Equivalent thermal conductivity coefficient of heat pipe	3000 W/(m·°C)	1000–10,000 W/(m·°C)

environment. The heat-dissipating plate is set on the instrument's back to dissipate the heat generated by the heating components. The resistance heating plate is pasted at the key positions of the detector and optical element to compensate for the heat loss under low-temperature conditions so that the temperature of the whole structure is balanced within the working temperature range.

5.2. Thermal FEM description

The temperature of the photodetector is the most crucial part of the instrument. As the thermal equilibrium around the instrument (Fig. 4), heat is mostly generated around the detector and radiated from the heat-dissipating plate to the cold black space through each interface. There is also heat exchange between structural components and MLI. A small amount of heat enters the cold black space through MLI.

Generally, thermal conductivity coefficient of each interface is much smaller than that of the material and is greatly affected by the contact state. The order of magnitude for contact heat-transfer coefficient is 10^2 W/(m^2·°C) ~10^3 W/(m^2·°C). The thermal conductivity coefficients (x1-x7) between interfaces occupies a certain range (Table 1). x8 and x9 are the active heating power for detectors, which in practice tend to fluctuate. x10~x14 depends on the material properties, which vary with product batches. x15 is the equivalent thermal conductivity coefficient of the heat pipe. The heat pipe is filled with multiphase material, so the coefficient is not a certain value either. MLI is simplified into a two-layer structure to simulate its heat transfer with the ambient environment. The equivalent thermal radiation coefficient is 0.03 between the two layers [34]. The coefficient is so small that the temperature distribution doesn't change with the variation of this coefficient. Optimization of this coefficient is excluded. Selection of the initial value and range of each parameter, please refer to Refs. [30,35].

The finite element model of the solar spectrometer was established in UG NX according to the 3D model of the instrument, as shown in Fig. 5. Since the components of the solar spectrometer are mostly thin-walled structures, shell elements were used to represent structures with the equivalent thickness. The density of the grid was divided to reflect the degree of concern. Heat transfer of the interface was expressed as "thermal couple", and corresponding thermal conductivities were given to each "couple". The whole instrument thermal model was divided into 8395 grid cells, and 38 thermal couplings were established.

Thermal conductivity coefficient of interface, heat power, and material thermal properties along heat transfer path are listed in Table 1 with the initial value of x1~x15. After the FEM was established, the environmental boundary condition, which is the low-temperature condition, was applied to the thermal FEM. The FEM was solved by the spatial thermal analysis solver in NX, which integrates the view factor calculation technology. The calculated temperature distribution program is shown in Fig. 6.

There are 8 temperature measuring positions corresponding to T1~T8 in Fig. 4. Moreover, Table 2 shows the comparison between the temperatures simulated and those in the thermal equilibrium experiment.

As shown in Table 2, there was a big difference between the measured temperature and the simulated ones at each temperature measuring position. In addition, the maximum temperature difference at T5 was about 10 °C. The main reason is that the x1~x15 parameters are

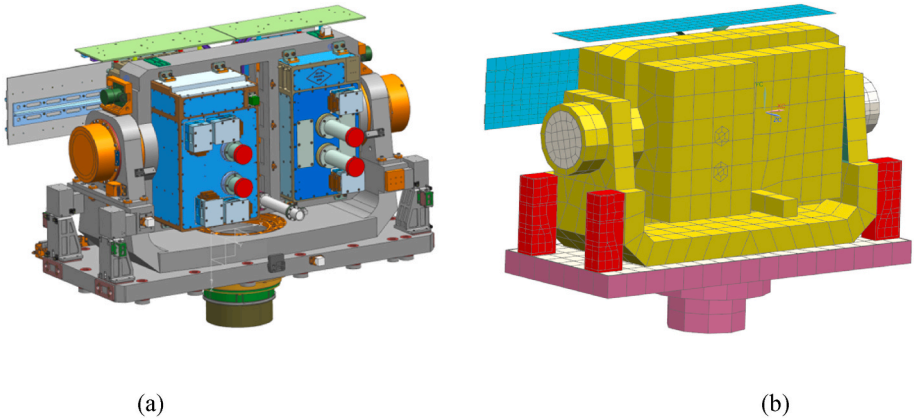

(a) (b)

Fig. 5. Finite element modeling of Solar spectrometer. (a) 3D model of Solar spectrometer; (b) FEM of the solar spectrometer.

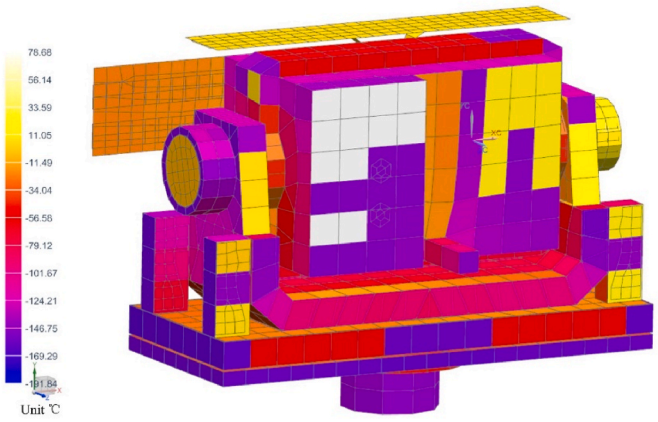

Fig. 6. Simulated temperature distribution of the space-borne instrument.

empirical or estimated values, which differed from the experimental ones. Usually, the true values of the parameters are too difficult to measure. Therefore, the parameters need to be updated.

5.3. Sensitivity analysis of parameters

The mathematical model between the parameters and the temperature response was established in the form of the Kriging model. Before that, sensitivity analysis was used to select the parameters to reduce the time of modeling and model updating.

Sensitivity analysis refers to changing only one parameter at a time while other parameters remain unchanged. Within the possible variation range of the parameters (Table 1), five levels were evenly selected, and the corresponding response was calculated in thermal FEM.

Fig. 7 shows the calculation results of every temperature measuring position when each parameter changes separately. It can be seen that the influence of parameter variation on temperature is monotonic. Taking Fig. 7(a) as an example, the influence of x10 on T1 was the most severe; there was a temperature change of 14 °C in the scope of parameters.

If a parameter has no or low influence on the temperature, the parameter does not contribute to the model and should be eliminated. Given that the influence of parameters on temperature is monotonous, we first calculated the temperature changes caused by a certain parameter at a certain position as $(T_{max} - T_{min})$ in eq. (13), and then summarized the temperature changes of all positions (temperature difference of 8 positions).

$$P_{xi} = \sum_{1}^{8} (T_{max} - T_{min}) \tag{13}$$

P_{xi} is the comprehensive influence degree of the parameter on the temperature response. As shown in Fig. 8, x4, x11, x13, and x14 are below the criteria red line, 1 °C, which means they are not sensitive to temperature response and should be eliminated.

5.4. Modeling process

Eleven design parameters were taken as the variables in the second step of DOE. The lower bound and upper bound were the same as those in sensitivity analysis listed in Table 1. The design matrix of the DOE was generated based on the bounds by using the Latin Hypercube Sampling method. Sixty-six sampling points were obtained after DOE.

Because the Kriging model has only one response, the temperature at each measuring position could be used to generate a model. A total of 8 Kriging models corresponding to T1~T8 were obtained. The values of θ in each model are shown in Table 3.

Mat-lab automatically calculated the θ value of the model after inputting the initial value, value range, and corresponding parameters by using the DACE toolbox.

The accuracy of the constructed Kriging metamodels needs to be assessed before model updating. If the output values of Kriging models are close enough to those calculated in FEM under the same parameters, the models are considered accurate. Since a Kriging model goes through all the training points, LHS is required to generate another 5 sampling points as the checking points.

Root Mean Square Error (RMSE) is an appropriate method to evaluate the accuracy of the Kriging model, which is defined as:

$$RMSE = \sqrt{\frac{\sum_i (T_{ki} - T_i)^2}{n}} \tag{14}$$

where T_{ki} is response temperature of i-th Kriging model at checking points and T_i is the corresponding simulated temperature of FEM; n is

Table 2
Temperature comparison at every temperature measuring position.

Thermocouple	T1	T2	T3	T4	T5	T6	T7	T8
Experiment (°C)	13.5	8.0	8.4	8.3	14.7	−8.2	−15	2.0
Simulation (°C)	15.48	10.26	11.2	10.17	24.23	−6.99	−13.49	4.75

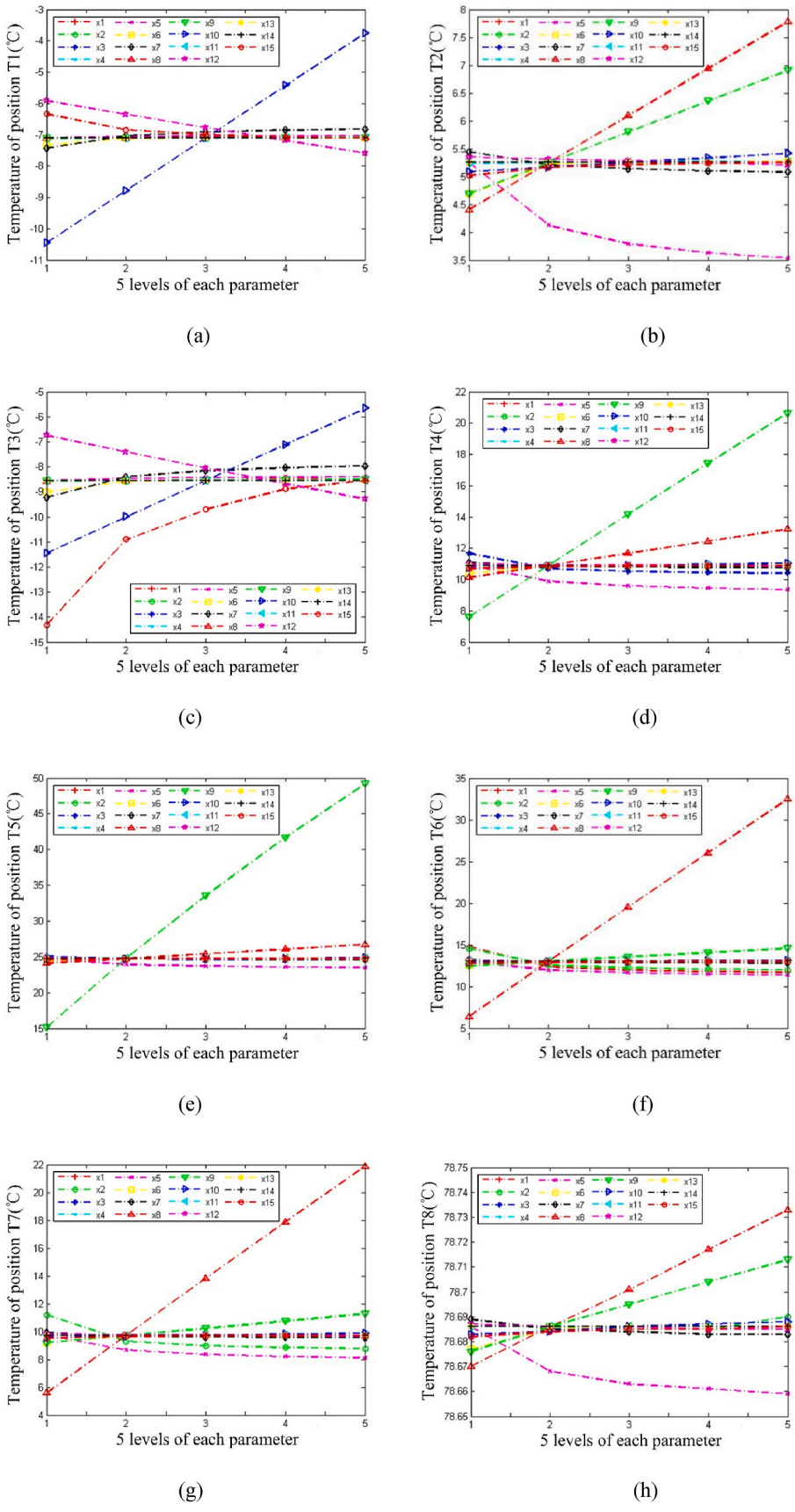

Fig. 7. Sensitivity analysis of parameters in thermal FEM. (a) parameter influences at position T1; **(b)** parameter influences at position T2; **(c)** parameter influences at position T3; **(d)** parameter influences at position T4; **(e)** parameter influences at position T5; **(f)** parameter influences at position T6; **(g)** parameter influences at position T7; **(h)** parameter influences at position T8.

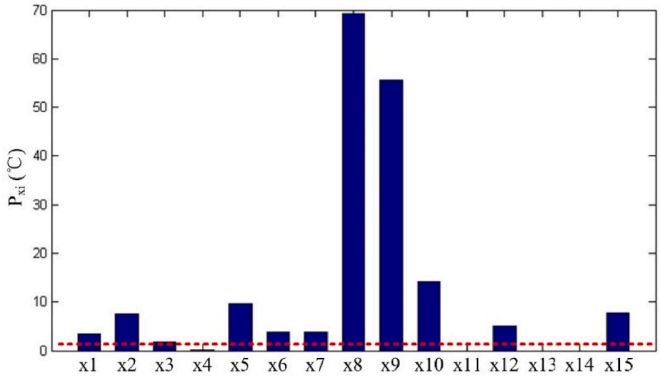

Fig. 8. Parameters effecting the temperature.

the number of the checking points. Temperature comparison between Kriging models and FEM is shown in Fig. 9 and Table 4. The maximum RMSE was 0.45 °C, which is less than 1 °C, thus suggesting that the Kriging models are accurate enough to represent the thermal FEM.

5.5. Model updating

The Kriging model is constructed to substitute FEM in the model updating process. Eleven selected parameters were the variables, which needed to be updated. Variable scopes were taken as same as the DOE variable bounds, and GA was used to solve the optimization problem. As mentioned in Chapter 4, the objective function is the difference between the Kriging response and experimental data. The optimal results of the input variables shown in Table 5 were obtained after 150 iterations. The percent changes of the variables are also given in Table 5.

x1∼x7 are the contact thermal coefficient conductivity coefficient of the interface in Table 5. Since contact thermal conductivity coefficient could only be roughly determined by the contact area and surface roughness in thermal simulation analysis, the numerical values of x1∼x7 greatly changed as the model updated. The equivalent thermal conductivity coefficient of the heat pipe x15 also changed to 1167 W/(m·°C) after the model was updated. x12 is the surface emissivity of the material, which has a small impact on the instrument temperature distribution.

6. Discussion

In order to verify the effectiveness of the model updating, the updated parameters were brought into the Kriging model and FEM. Fig. 10 shows the responded temperature values (blue bars and cyan bars). Compared with the initial temperature (red bars) at each measuring position, the simulated temperature values have a better agreement with the experimental data (green bars).

The calculation results of Kriging and FEM were similar (the maximum temperature difference was 1.2 °C), which further confirmed the accuracy of the Kriging model. After the model parameters were updated, the temperature values of all temperature measuring positions significantly changed. T5, which had the most drastic temperature change, drooped from 24 °C to 14 °C, as shown in Table 6. RMSE of temperature deviation from experiment for the updated model was 0.88 °C and 3.97 °C for models before updating.

Fig. 10 shows that the simulated temperature before parameter

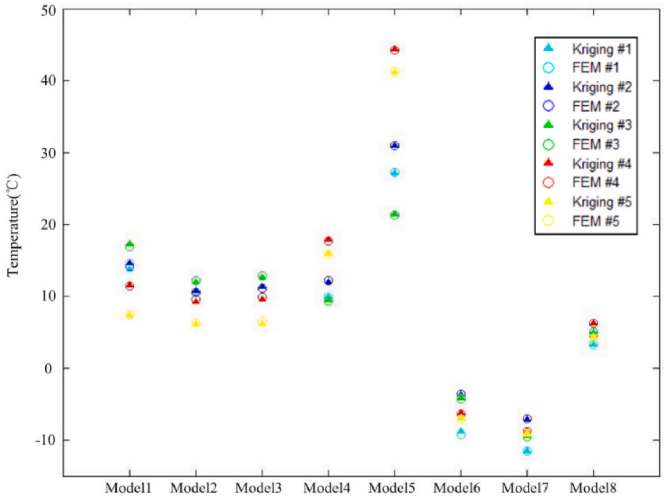

Fig. 9. Responses of Kriging models and FEM at checking points.

Table 5
Updated parameters of FEM.

Parameters	Unit	Initial value	Lower bound	Upper bound	Optimized value	Percent change
x1	W/°C	2.3	0.5	10.0	1.7	−26.09%
x2	W/°C	5.0	0.5	15.0	12	140.00%
x3	W/°C	5.0	0.5	15.0	12.7	154.00%
x5	W/°C	4.0	0.5	15.0	8.3	107.50%
x6	W/°C	1.0	0.2	5.0	1.1	10.00%
x7	W/°C	1.0	0.6	8.0	3.7	270.00%
x8	W	6.0	4.0	8.0	5.5	−8.33%
x9	W	2.0	1.0	3.0	1.1	−45.00%
x10	°C	−4.0	−8.0	−2.0	−6.3	57.50%
x12	–	0.88	0.6	0.98	0.96	9.09%
x15	W/(m·°C)	3000	1000	10,000	1167	−61.10%

Table 3
θ values of 8 Kriging models.

	θ1	θ2	θ3	θ4	θ5	θ6	θ7	θ8	θ9	θ10	θ11
Model 1	3.56E-02	1.10E-02	6.45E-03	1.10E-02	1.72E-04	1.30E-03	9.17E-02	3.96E-02	1.68E-07	4.21E-03	1.83E-05
Model 2	7.66E-03	8.44E-02	2.93E-03	1.90E-02	1.12E-03	3.83E-03	1.36E-01	5.87E-03	3.09E-03	6.19E-03	1.82E-03
Model 3	7.26E-03	8.90E-02	2.78E-03	9.48E-03	1.07E-03	1.01E-03	1.29E-01	1.91E-03	2.02E-03	5.87E-03	2.64E-03
Model 4	3.63E-04	1.00E-03	7.19E-03	6.13E-03	4.04E-04	3.03E-02	2.23E-03	1.16E-02	6.89E-04	5.00E-04	8.61E-05
Model 5	3.63E-04	6.53E-04	8.52E-04	2.11E-03	6.19E-04	5.27E-04	9.48E-04	1.16E-02	1.01E-04	4.79E-05	1.32E-04
Model 6	1.24E-03	8.30E-04	4.69E-03	4.62E-04	1.24E-03	9.64E-03	1.23E-02	7.46E-04	2.66E-02	2.48E-03	5.97E-03
Model 7	2.93E-04	5.00E-04	6.59E-05	1.25E-04	3.48E-05	5.45E-02	1.31E-03	2.37E-04	9.39E-03	1.23E-02	1.15E-01
Model 8	7.26E-03	3.83E-03	2.02E-03	9.39E-02	5.62E-04	8.99E-03	8.99E-03	7.26E-03	2.37E-03	1.07E-03	2.66E-04

Table 4
RMSE of Kriging models.

	Model 1	Model 2	Model 3	model 4	model 5	Model 6	Model 7	Model 8
RMSE (°C)	0.4548	0.1688	0.3184	0.0962	0.0583	0.2065	0.1067	0.0421

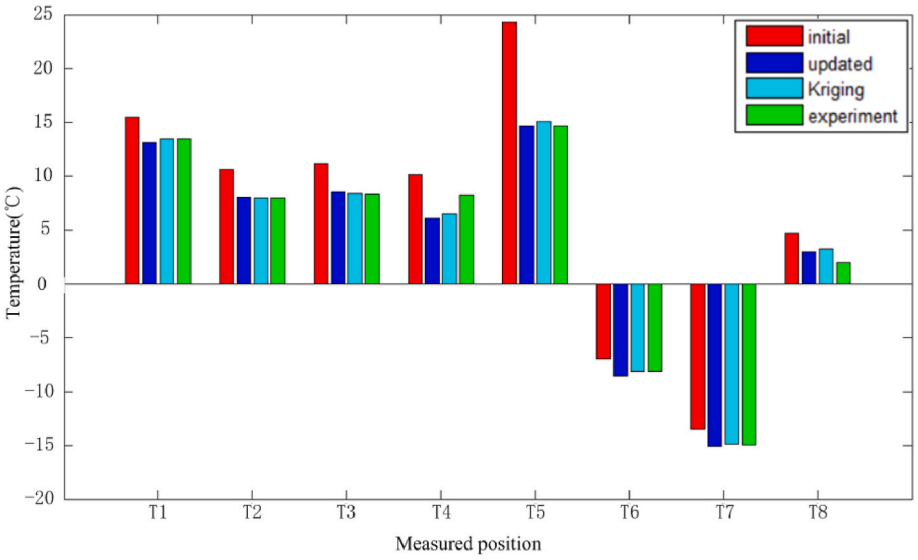

Fig. 10. Temperature changes of different models under low temperature condition.

Table 6
Temperature change under low temperature condition.

	Initial (°C)	Updated (°C)	Kriging (°C)	Experiment (°C)	Temperature change after model updating (%)
T1	15.5	13.15	13.51	13.5	−15%
T2	10.6	8.04	7.99	8.0	−24%
T3	11.2	8.57	8.43	8.4	−23%
T4	10.2	6.11	6.54	8.3	−40%
T5	24.3	14.69	15.07	14.7	−39%
T6	−7.0	−8.57	−8.12	−8.1	22%
T7	−13.5	−15.08	−14.89	−15.0	12%
T8	4.8	3.02	3.28	2.0	−37%

updating was higher than that in the heat balance experiment. After updating, temperatures at all temperature measuring positions decreased to a different degree, which was mainly related to the structural heat leakage. Although the instrument's surface is wrapped with thermal insulation material, the heat loss at some overlapping positions was unavoidable. However, the ideal structure of FEM model cannot simulate this kind of heat leakage. Therefore, there was an increase in the emissivity of the heat-dissipating plate after the model was updated, which equivalently compensated for the heat loss. Moreover, the change in the interface contact thermal resistance led to different temperature drops.

In order to further demonstrate the correctness of model updating, high-temperature boundary conditions were applied to the FEM model to calculate the temperature response. Temperatures of measuring positions before and after model updating are compared in Fig. 11. The comparison of temperature data is shown in Table 7.

Same as in low-temperature conditions, model updating made the FEM calculation results closer to thermal equilibrium experimental results. RMSE of temperature deviation of initial simulated temperatures from the measured ones was 3.55 °C. After model updating, RMSE decreased to 1.11 °C, which was a big improvement in the accuracy of the thermal FEM. Similarly, the phenomenon of temperature dropped after model updating appeared in high-temperature conditions.

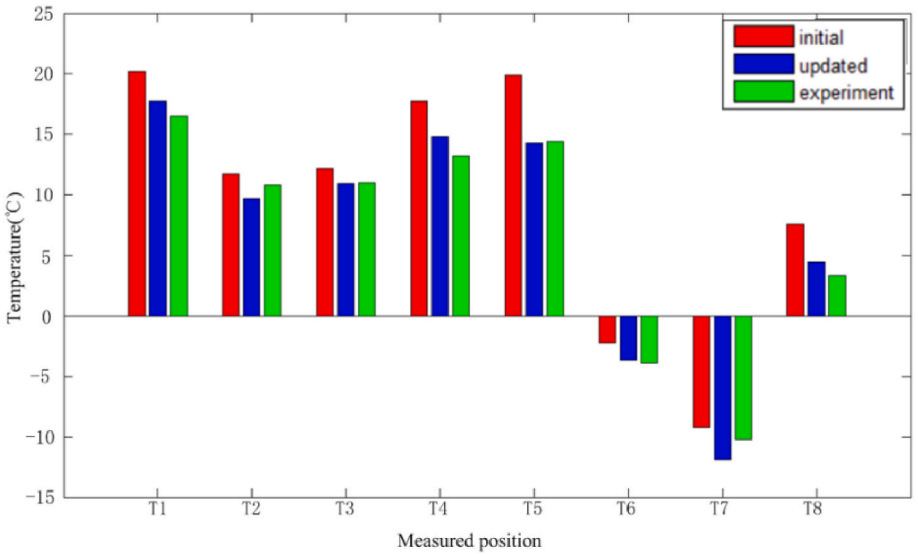

Fig. 11. Temperature changes of different models under a high temperature condition.

Table 7
Temperature change under high temperature condition.

	Initial (°C)	updated (°C)	experiment (°C)	Temperature change after model updating (%)
T1	20.19	17.76	16.5	−12%
T2	11.76	9.67	10.8	−17%
T3	12.19	10.93	11	−10%
T4	17.74	14.86	13.2	−16%
T5	19.89	14.29	14.4	−28%
T6	−2.24	−3.67	−3.9	64%
T7	−9.19	−11.87	−10.2	29%
T8	7.62	4.46	3.3	−41%

7. Conclusion

In the present study, we used metamodel techniques as a fast-running model to facilitate the application of mathematical algorithms in model updating. The Kriging model was introduced as the metamodel to replace the computational expensive thermal FEM during the optimization process. According to the characteristics of the thermal FEM, we proposed a two-step DOE method, which removes the invalid parameters and improves the modeling efficiency. Sensitivity analysis in the first step determined the influence degree of the parameters. Eight kriging models constructed in the second step resulted as highly consistent with FEM.

A significant improvement in temperature predicting accuracy was achieved after the model was updated. The updated parameters of the model were evaluated under two working conditions. Under low-temperature conditions, the RMSE of temperature deviation from the experiment was 0.88 °C and 3.97 °C after and before updating. For high-temperature conditions, RMSE drooped from 3.55 °C to 1.11 °C after updating. Moreover, the model updating compensated for the heat leakage of the system, and the temperature distribution was more consistent with the experimental results. The proposed method can be successfully used for the model updating of thermal FEM of the space instrument.

Declaration of competing interest

The authors declare that they have no known competing financial interests or personal relationships that could have appeared to influence the work reported in this paper.

Data availability

Data will be made available on request.

Acknowledgments

This work was supported by the Science and Technology Development Program of Jilin Province (No. 20200403060SF).

References

[1] Chen Zheng, Jianhua Qi, Jing Fu, et al., Thermal analysis on alpha magnetic spectrometer main radiators under the flight attitude adjustment of international space station, Appl. Therm. Eng. 164 (2020) 114457.
[2] Ai Ueno, Yuji Suzuki, Design and analysis of micro thermal switch using the near-field effect for space applications, Int. J. Therm. Sci. 132 (2018) 161–167.
[3] G.R. Min, Satellite Thermal Control Technology, Aerospace Press, Beijing, 1991, pp. 34–35.
[4] V. Mareshi, V. Perotto, M. Gorlani, Thermal test correlation with stochastic technique, SAE Int. (2005), 01-2855.
[5] W.L. Cheng, N. Liu, Z. Li, et al., Application study of a correction method for a spacecraft thermal model with a Monte-Carlo hybrid algorithm, Chin. Sci. Bull. (2010) 55.
[6] Q. Li, L.H. Chen, Correction for transient thermal analysis model of Carbon Dioxide detector, Chin. Space Sci. Technol. 37 (2017) 44–52.
[7] X.B. Ke, Research on the Construction and Optimization Algorithm for Kriging Model, M.D Thesis, XiDian University, 2015, pp. 10–20.
[8] Z.J. Huang, C.G. Wang, J. Chen, et al., Optimal design of turbine disc based on Kriging surrogate models, Comput. Struct. 89 (2011) 27–37.
[9] T.Z. Li, X.L. Yang, An efficient uniform designing for Kriging-based response surface method and its application, Comput. Geotech. 109 (2019) 12–22.
[10] J.T. Wang, C.J. Wang, J.P. Zhao, Frequency response function-based model updating using Kriging model, Mech Syst Signal 87 (2017) 218–228.
[11] D.S. Shan, Q. Li, I. Khan, et al., A novel finite element model updating method based on substructure and response surface model, Eng. Struct. 103 (2015) 147–156.
[12] J. Sacks, W.J. Welch, T.J. Mitchell, et al., Design and analysis of computer experiments, Stat. Sci. 4 (1989) 409–435.
[13] A. Giunta, L.T. Watson, A comparison of approximation modeling techniques: polynomial versus interpolating models, proceedings of the 7th AIAA/USAF/NASA/ISSMO symposium on multidisciplinary analysis and optimization (1998).
[14] A.J. Brooker, Design and Analysis of Computer Experiments, Proceedings of the 7th AIAA/USAF/NASA/ISSMO Symposium on Multidisciplinary Analysis and Optimization, 1998.
[15] I.G. Osio, C.H. Amon, An engineering design methodology with multistage Bayesian surrogates and optimal sampling, Res. Eng. Des. 8 (1996) 189–206.
[16] T. Ishimoto, H.M. Pan, Thermal network correction techniques, AIAA70 821 (1970).
[17] S. Shimoji, K. Oshima, A new thermal network correction method by the statistical regression analysis, AIAA 78-882 (1978).
[18] J.H. Weng, Z.F. Pan, A correction method for spacecraft thermal network and its coefficients, Chin. Space Sci. Technol. 4 (1995) 10–14.
[19] J.Y. Zhang, H.P. Chang, L.G. Wang, Correction method for transient thermal analysis model of small satellite, Chin. Space Sci. Technol. 4 (2013) 24–30.
[20] P. Goovaerts, Geostatistics for Natural Resources Evaluation, Oxford University Press, New York, 1997.
[21] A.G. Journel, C.J. Juijbregts, Mining Geostatistics, Academic Press, New York, 1978.
[22] D.B. Ripley, Spatial Statistics, John Wiley & Sons, Inc., New York, 1981.
[23] N.A.C. Cressie, Statistics for Spatial Data, John Wiley & Sons, Inc., New York, 1991.
[24] T.W. Simpson, M. Mauery, J.J. Korte, et al., Kriging models for global approximation in simulation-based multidisciplinary design optimization, AIAA J. 39 (2001) 2233–2241.
[25] J.D. Martin, T.W. Simpson, A study on the use of Kriging models to approximate deterministic computer models, in: Computers and Information in Engineering Conference, 2003.
[26] S.E. Gano, J.E. Renaud, J.D. Martin, et al., Update strategies for Kriging models for use in variable fidelity optimization, Struct. Multidiscip. Optim. 32 (2005) 287–298.
[27] J.D. Martin, T.W. Simpson, On the use of Kriging models to approximate deterministic computer models, in: Proceedings of the ASME 2004 International Design Engineering Technical Conferences and Computers and Information in Engineering Conference, American Society of Mechanical Engineers, 2004.
[28] J.D. Martin, T.W. Simpson, Use of Kriging Models to Approximate Deterministic Computer Models, ASME 2003 Design Engineering Technical Conferences and Computers and Information in Engineering Conference, 2003.
[29] S. Pradhan, S.V. Modak, Normal response function method for mass and stiffness matrix updating using complex FRFs, Mech. Syst. Signal Process. 32 (2012) 232–250.
[30] L. Guo, Q.W. Wu, C.X. Wang, Sensitivity analysis of thermal design parameters for focal plane assembly in a space spectral imaging instrument, Heat Mass Tran. 49 (2013) 299–308.
[31] M.D. McKay, W.J. Conover, R.J. Beckman, A comparison of three methods for selecting values of input in the analysis of output from a computer code, Technometrics 21 (1979) 239–245.
[32] M. Miki, T. Hiroyasu, M. Kaneko, et al., A parallel genetic algorithm with distributed environment scheme, IEEE Int. Conf. Syst. Man Cybern. 1 (1999).
[33] L. Chen, Y. Hou, L. Xi, Calibration of copper-constantan thermocouple and related error analysis, Cryogenics 166 (2008) 18–23.
[34] J.S. Jiang, Multilayer insulation materials and their application to spacecrafts, Aerospace Mater. Technol. 4 (2000) 17–25.
[35] L. Guo, Q.W. Wu, C.X. Yan, et al., Thermal analysis and verification of CCD components in spectral imagers at steady and transient states, Opt. Prec. Eng. 11 (2010) 2375–2382.